

# Feedback-controlled laser ablation for cancer treatment: comparison of On-Off and PID control strategies \*

A. Orrico, *Student Member, IEEE*, Sanzhar Korganbayev, *Student Member, IEEE*, Leonardo Bianchi, *Student Member, IEEE*, Martina De Landro, *Student Member, IEEE*, Paola Saccomandi *Senior Member, IEEE*

**Abstract**—Laser ablation is a rising technique used to induce a localized temperature increment for tumor ablation. The outcomes of the therapy depend on the tissue thermal history. Monitoring devices help to assess the tissue thermal response, and their combination with a control strategy can be used to promptly address unexpected temperature changes and thus reduce unwanted thermal effects. In this application, numerical simulations can drive the selection of the laser control settings (i.e., laser power and gain parameters) and allow evaluating the thermal effects of the control strategies.

In this study, the influence of different control strategies (On-Off and PID-based controls) is quantified considering the treatment time and the thermal effect on the tissue. Finite element model-based simulations were implemented to model the laser-tissue interaction, the heat-transfer, and the consequent thermal damage in liver tissue with tumor. The laser power was modulated based on the temperature feedback provided within the tumor safety margin. Results show that the chosen control strategy does not have a major influence on the extent of thermal damage but on the treatment duration; the percentage of necrosis within the tumor domain is 100% with both strategies, while the treatment duration is 630 s and 786 s for On-Off and PID, respectively. The choice of the control strategy is a trade-off between treatment duration and unwanted temperature overshoot during closed-loop laser ablation.

**Clinical Relevance**— This work establishes that different temperature-based control of the laser ablation procedure does not have a major influence on the extent of thermal damage but on the duration of treatment.

## I. INTRODUCTION

Thermotherapy techniques are largely employed as a clinical procedure to treat unresectable tumors [1]. The application of laser technology is increasingly being used as a minimally invasive local treatment to induce thermal necrosis on cancerous tissue since it can minimize operative trauma and reduce healing time [2].

The laser light brought through the laser tip inside the target area is converted into thermal energy. The subsequent temperature increase induced has a different biological effect. Temperatures that are ranging from 60 °C to 100 °C could provoke protein denaturation, and temperatures above 100 °C

may lead to bio-tissue carbonization. Above 42.5 °C, healthy cells are generally less sensitive to hyperthermia than tumor cells [3], [4]. The effectiveness of laser therapy depends on the thermal history in the tumor tissue and the surrounding healthy tissue [5]. Real-time temperature monitoring has been considered decisive in thermotherapy treatments since the temperature feedback could be used to adjust the laser setting parameters and treatment duration [6]. Several studies investigated the usage of sensors [7]–[11] or temperature imaging techniques [12] to provide real-time temperature monitoring during the laser ablation treatment. To improve the treatment therapeutic effectiveness, some researchers have recently exploited the provided temperature feedback to implement a closed-loop approach to modulate the delivery of laser energy [13], [14]. The most commonly used closed-loop approaches are based on the On-Off control strategy [15], which intermittently delivers the power, or based on the Proportional-Integrative-Derivative (PID) control strategy [16], which instead modulates the laser irradiance. Presently, there is not a clear indication of the best approach to be used for implementing an effective closed-loop control, and the effect of controlling parameters on the tissue thermal damage is still under investigation [15]. For this reason, in this work, we study the influence of different control strategies on the treatment duration, temperature overshoot and the provoked thermal damage by exploiting theoretical models.

## II. MATERIALS AND METHODS

The heat distribution in a cancer liver tissue undergoing laser treatment and the consequent thermal damage were modeled employing COMSOL Multiphysics 5.5 software (COMSOL, Inc., Burlington, MA, USA). The following sections describe the different steps to construct the model in COMSOL Multiphysics.

### A. Geometry

A two-dimensional axisymmetric (along the y-axis) model was used to mimic the behavior of the liver tumor and the adjoining healthy tissue. The geometry of one symmetrical part of the model is reported in Fig. 1. The domain with the physical properties of the liver has been represented with a cylinder of 50 mm of radius and 50 mm of thickness. Inside

\* This project has received funding from the European Research Council (ERC) under the European Union's Horizon 2020 research and innovation programme (Grant agreement No. 759159).

A. Orrico, S. Korganbayev, L. Bianchi, M. De Landro and P. Saccomandi Authors are with the Department of Mechanical Engineering, Politecnico di

Milano, 20156 Milano, Italy (e-mail: annalisa.orrico@polimi.it, sanzhar.korganbayev@polimi.it, leonardo.bianchi@polimi.it, martina.delandro@polimi.it, corresponding author e-mail: leonardo.bianchi@polimi.it).

the cylinder, the circle and its outer ring have been inserted to represent the liver tumor and the safety margin [17], respectively. Safety margins have been inserted, as heat treatment is considered effective when the tumor is destroyed and less than 5% of the surrounding healthy tissue is thermally damaged [18], [19]. To reach this condition, the temperature has been controlled  $T_{con}$  within the safety margin and closer to the tumor (red dot in Fig.1). In our study, a safety margin of 5 mm has been chosen for a 20 mm-diameter liver tumor.

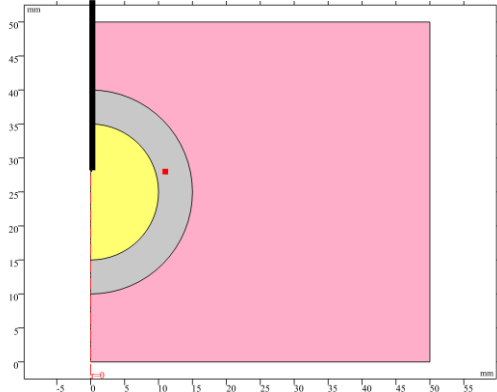


Fig. 1. Geometry of the axisymmetric computational model: tumor (yellow), safety margin (gray) and healthy tissue (pink). The laser fiber (black line) is positioned at  $x=0$ .

### B. Laser light energy

The physical phenomenon underlying the laser ablation is the photothermal conversion of near-infrared laser light absorbed by biological components. The laser light is delivered through a fiber optic tip inside the tumor. The interaction between the biological media and the NIR irradiation has been modeled with the Beer-Lambert law. According to the Beer-Lambert law, the laser light absorption inside biological tissue is affected by absorption and scattering phenomena, in the following way [20]:

$$Q_{Laser} = \mu_{eff} \cdot I(r) \cdot e^{-\mu_{eff} \cdot z} \quad (1)$$

where  $\mu_{eff}$  ( $m^{-1}$ ) represents the effective attenuation coefficient that takes into account the absorption and the scattering contributions,  $z$  (m) is axial distance from the laser source in the direction of laser light, and  $I(r)$  ( $W \cdot m^{-2}$ ) is the irradiance applied at the interaction surface with the laser tip.  $I(r)$  can be expressed with the following equation:

$$I(r) = I_0 \cdot e^{-\frac{r^2}{2\sigma^2}} \quad (2)$$

where  $r$  (m) represents the radial distance from the laser applicator,  $\sigma$  (m) is the standard deviation of the laser beam and  $I_0$  ( $W \cdot m^{-2}$ ) is the maximum value of irradiation intensity applied.  $I_0$  can be calculated with (3):

$$I_0 = \frac{P}{2 \cdot \pi \cdot \sigma^2} \quad (3)$$

where  $P$  (W) is the value of the laser power. The choice of the control strategy will directly affect the laser power, and indirectly the heat distribution inside the biological tissue.

### C. Thermal distribution and thermal damage

The bio-heat equation used to predict the spatial-temporal temperature distribution in the biological tissue is the Pennes' equation (4) and (5), based on Fourier's law [21]. The following equations have been used to predict the heat distribution in the liver tumor (under script t) and the healthy liver (under script h) respectively:

$$\rho_t \cdot c_{p_t} \cdot \frac{\partial T_t}{\partial t} = k_t \cdot \nabla^2 T_t + Q_{laser} \quad (4)$$

$$\rho_h \cdot c_{p_h} \cdot \frac{\partial T_h}{\partial t} = k_t \cdot \nabla^2 T_h \quad (5)$$

where the left-hand-side denotes the time-dependent term, and it takes into account the tissue density  $\rho$  ( $kg \cdot m^{-3}$ ), the tissue heat capacity  $c_p$  ( $J \cdot kg^{-1} \cdot K^{-1}$ ) and the tissue temperature  $T$  (K). The first term of the right-hand-side represents the heat conduction that depends on the tissue thermal conductivity  $k$  ( $W \cdot m^{-1} \cdot K^{-1}$ ). The last term in (4) is the heat generation  $Q_{laser}$  ( $W \cdot m^{-3}$ ) due to the laser-tissue interaction.

The thermal damage can be predicted by the Arrhenius model (6), which establishes the degree of injury  $\Omega$  as a function of temperature and the exposure time [22].

$$\Omega(t) = \int_0^t A \cdot e^{-\frac{E_a}{R \cdot T}} \cdot dt \quad (6)$$

where  $A$  ( $s^{-1}$ ) is the frequency factor,  $E_a$  ( $J \cdot mol^{-1}$ ) denotes the activation energy for an irreversible damage reaction,  $R$  ( $J \cdot K^{-1} \cdot mol^{-1}$ ) is the universal gas constant. The optical parameters of the model can be found in [23], the thermal and the kinetic parameters in [9].

### D. Control strategies

In this work, we investigate the effects of different control strategies. The chosen control strategy sets the deposited laser power, and given the equations seen above, it has an indirect effect on the laser ablation treatment. For both control strategies, it was decided to stop laser ablation treatment when the mean value of the degree of injury within the safety margin reaches a value of 0.8 [17] or in the scenario in which the maximum recorded temperature in the same area exceeds a value of 150 °C. The first condition ensures obtaining the destruction of the cells within the tumor, while the second equation is used as a precautionary measure to avoid unwanted thermal effects on surrounding healthy tissue. To simulate a plausible scenario, the control algorithm is activated at regular time instants; in our case, it is chosen to update the laser power every 0.5 s. The temperature threshold  $T_{th}$  is set to 60 °C.

In the On-Off control strategy, the power is always delivered at the same value or not deposited at all. When the temperature measured in the control point (red dot in Fig. 1) exceeds the threshold temperature, the laser beam delivery is suspended until the temperature is below the threshold. Two power values were chosen for our experiments: the minimum power  $P_{min} = 1.75$  W and the maximum power of  $P_{max} = 6.56$  W.

Using the PID control strategy, the power delivered by the laser source is governed by the following equation:

$$P(t) = k_p(T_{th} - T_{con}) + k_d \frac{d(T_{th} - T_{con})}{dt} + k_i \int_0^t (T_{th} - T_{con}) dt \quad (7)$$

where  $k_p [W \cdot K^{-1}]$  is the proportional gain,  $k_d [W \cdot s \cdot K^{-1}]$  the derivative gain and  $k_i [W \cdot s^{-1} \cdot K^{-1}]$  denotes the integrative gain,  $T_{th}$  is threshold temperature (60 °C),  $T_{con}$  is controlled temperature. The power range that can be delivered is from  $P_{min} = 1.75$  W and  $P_{max} = 6.56$  W. In our experiments, two different combination of gain parameters were tested:  $PI_1$  with  $k_p = 0.77 W \cdot K^{-1}$  and  $k_i = 0.0065 W \cdot s^{-1} \cdot K^{-1}$  then  $PI_2$  with  $k_p = 0.77 W \cdot K^{-1}$  and  $k_i = 0.0042 W \cdot s^{-1} \cdot K^{-1}$ . The derivative gain was set to  $k_d = 0$  in both cases, as published in [16].

The power delivered for the described control strategies is shown in Fig. 2.

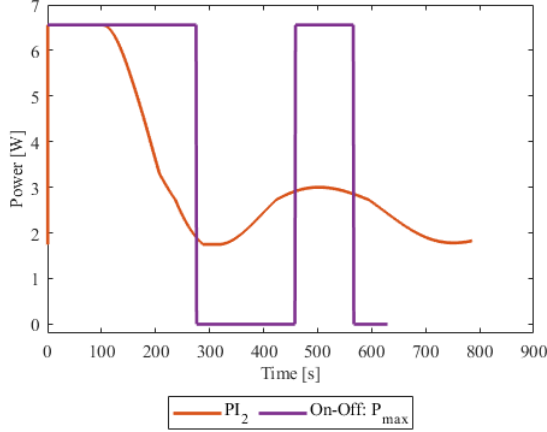


Fig. 2. Power profiles for  $PI_2$  ( $k_p = 0.77 W \cdot K^{-1}$  and  $k_i = 0.0042 W \cdot s^{-1} \cdot K^{-1}$ ) and On-Off:  $P_{max}$  control strategies.

### III. RESULTS

The chosen threshold temperature was set to 60 °C because it corresponds to an instantaneous thermal injury. Fig. 3 shows the temperature profiles at the control position (red dot in Fig. 1); it can be seen how different control strategies affect the treatment time. In the case of the On-Off control strategy at maximum power (purple line), the treatment time is shorter ( $t \sim 630$  s), but the temperature overshoot ( $\Delta T = 4.3$  °C), is quite high due to the delay of the tissue response. The effects of excessive temperature overshoot could propagate to the healthy region. On the other hand, in the case of the On-Off control strategy at minimum power (yellow line), the treatment exceeds the maximum duration of 15 minutes without reaching the temperature threshold, therefore without creating the expected thermal damage. In the case of the  $PI_1$  (blue line), the treatment time is comparable to the On-Off control strategy at maximum power and the temperature overshoot is almost  $\sim 3$  °C lower. Instead, the  $PI_2$  (red line) case shows an underdamped thermal response that lengthens the treatment times but leads to a negligible temperature overshoot. It can be seen as the choice of gain parameters strongly influences the temperature profile behavior; therefore, their choice must be accurate. The choice of control strategy affects the tissue thermal history, too. Fig. 4 reports the tissue temperature distribution of the different control strategies at different time instants. The temperature distributions before the switching off (left) and before the switching on (right) are shown at the top. Since the On-Off control strategy completely suspended the laser power delivery, we have a part of the treatment time in which the temperature distribution is governed by the heat

conduction, as is shown at the top right of Fig. 4. The bottom of Fig. 4 reports the thermal distributions of the  $PI_2$  control strategy when the overshoot occurs (left) and when the treatment time is approximately equal to  $\sim 450$  s. Although the PI control strategy shows temperature oscillations around the threshold temperature, the tissue thermal distribution does not experience an abrupt change as in the case of the on-off control strategy. Despite the temperature distribution strongly depends on the adopted control strategies, the final thermal damage does not show a significant variation in all domains (Table I) except for the On-Off at minimum power.

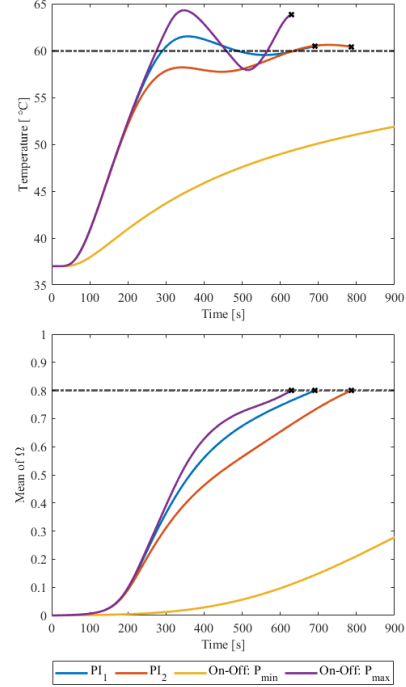


Fig. 3. Temperature profiles over time obtained for different control strategies (above). The average degree of injury within the safety margin over time for different control strategies (below).

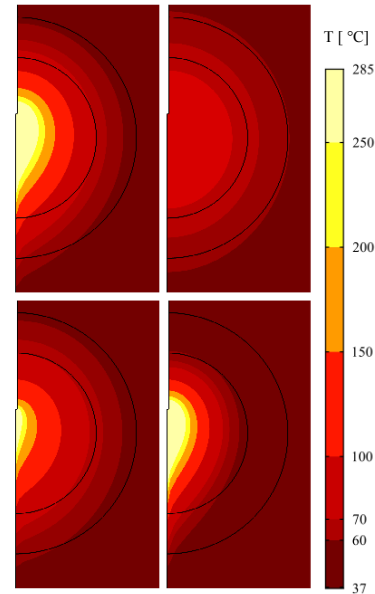


Fig. 4. Two-dimensional temperature distribution, in case of On-Off:  $P_{max}$  control strategy above, and in case of  $PI_2$  ( $k_p = 0.77 W \cdot K^{-1}$  and  $k_i = 0.0042 W \cdot s^{-1} \cdot K^{-1}$ ) control strategy below.

TABLE 1. SUMMARY OF THE MOST SIGNIFICANT RESULTS

	$PI_1$	$PI_2$	$On-Off:$ $P_{min}$	$On-Off:$ $P_{max}$
Time [s]	691.4	785.8	---	629.2
Necrosis in Tumor [%]	100	100	48.9	100
Necrosis in Margin [%]	17.9	15.6	0.9	22.9
Necrosis in Healthy Tissue [%]	0	0	0	0
Overshoot [°C]	1.52	0.61	---	4.30

To produce an average degree of injury equal to 0.8 in the safety margin domain (at bottom of Fig. 3), the different temperature distributions are compensated by the different treatment duration. Fig. 5 shows the thermal damage after the controls with On-Off at minimum power (on left) and with  $PI_2$  (on the right). Since the On-Off control strategy cannot change the delivered power value during the treatment, the selected power value could be not sufficient to produce the desired thermal damage within a reasonable treatment time, as it happened in Fig. 5.

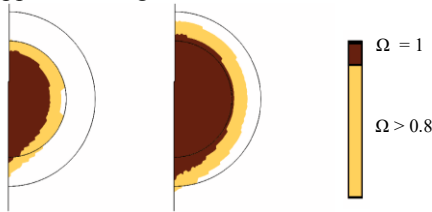


Fig. 5. Final thermal damage maps obtained with On-Off control strategy on the left and with the  $PI_2$  ( $k_p=0.77 \text{ W}\cdot\text{K}^{-1}$  and  $k_i=0.0042 \text{ W}\cdot\text{s}^{-1}\text{K}^{-1}$ ) control strategy on the right.

#### IV. CONCLUSION

In this study, we investigate the influence of different control strategies during controlled laser-induced thermotherapy. The On-Off control strategy has the advantage of being independent of the gain parameters. The absence of these parameters leads to a delay in the tissue thermal response caused by the heat conduction phenomenon; consequently, the On-Off control experiences a temperature overshoot that could become significant. The PI control strategy can address the delay of thermal response only when the gain parameters have been correctly defined. The choice of the control strategy is a trade-off between treatment duration and unwanted temperature overshoot during temperature-feedback laser ablation. Future works will be designed to experimentally assess the consequences of intermittent laser irradiation compared with continuous laser heating, from a biological point of view.

#### REFERENCES

- [1] J. Qian, "Interventional therapies of unresectable liver metastases," *J. Cancer Res. Clin. Oncol.*, vol. 137, no. 12, pp. 1763–1772, 2011.
- [2] K. Nagpal *et al.*, "Is minimally invasive surgery beneficial in the management of esophageal cancer? A meta-analysis," *Surg. Endosc.*, 2010.
- [3] J. J. Lagendijk and J. Mooibroek, "Hyperthermia treatment planning," *Recent Results Cancer Res.*, vol. 101, pp. 119–131, 1986.
- [4] M. Luo *et al.*, "Laser immunotherapy for cutaneous squamous cell carcinoma with optimal thermal effects to enhance tumour immunogenicity," *Int. J. Hyperth.*, vol. 34, no. 8, pp. 1337–1350, 2018.

- [5] Markolf H. Niemz, *Laser-tissue Interactions: Fundamentals and Applications*. Springer-Verlag, 2004.
- [6] P. Saccomandi, E. Schena, and S. Silvestri, "Techniques for temperature monitoring during laser-induced thermotherapy: An overview," *Int. J. Hyperth.*, vol. 29, no. 7, pp. 609–619, Nov. 2013.
- [7] D. S. Robinson *et al.*, "Interstitial Laser Hyperthermia Model Development for Minimally Invasive Therapy of Breast Carcinoma 11 This work was supported by Department of Defense Grant USAMRDC Log No. B4340289; by Cancer Link of the Sylvester Comprehensive Cancer Center, a breast c," *J. Am. Coll. Surg.*, vol. 186, no. 3, pp. 284–292, 1998.
- [8] P. J. Milne, J. M. Parel, F. Manns, D. B. Denham, X. Gonzalez-Cirre, and D. S. Robinson, "Development of stereotactically guided laser interstitial thermotherapy of breast cancer: In situ measurement and analysis of the temperature field in ex vivo and in vivo adipose tissue," *Lasers Surg. Med.*, 2000.
- [9] L. Bianchi, S. Korganbayev, A. Orrico, M. De Landro, and P. Saccomandi, "Quasi-distributed fiber optic sensor-based control system for interstitial laser ablation of tissue: theoretical and experimental investigations," *Biomed. Opt. Express*, vol. 12, no. 5, pp. 2841–2858, 2021.
- [10] A. Orrico, L. Bianchi, S. Korganbayev, M. De Landro, and P. Saccomandi, "Controlled photothermal therapy based on temperature monitoring: theoretical and experimental analysis," in *2021 IEEE International Symposium on Medical Measurements and Applications (MeMeA)*, 2021, pp. 1–6.
- [11] F. Morra *et al.*, "Spatially resolved thermometry during laser ablation in tissues: Distributed and quasi-distributed fiber optic-based sensing," *Opt. Fiber Technol.*, vol. 58, p. 102295, 2020.
- [12] M. De Landro *et al.*, "Fiber bragg grating sensors for performance evaluation of fast magnetic resonance thermometry on synthetic phantom," *Sensors (Switzerland)*, 2020.
- [13] T. H. Nguyen, S. Park, K. K. Hlaing, and H. W. Kang, "Temperature feedback-controlled photothermal treatment with diffusing applicator: theoretical and experimental evaluations," *Biomed. Opt. Express*, 2016.
- [14] S. Korganbayev *et al.*, "Closed-loop temperature control based on fiber bragg grating sensors for laser ablation of hepatic tissue," *Sensors (Switzerland)*, 2020.
- [15] S. Korganbayev, R. Pini, A. Orrico, A. Wolf, A. Dostovalov, and P. Saccomandi, "Towards temperature-controlled laser ablation based on fiber Bragg grating array temperature measurements," in *2020 IEEE International Workshop on Metrology for Industry 4.0 and IoT, MetroInd 4.0 and IoT 2020 - Proceedings*, 2020.
- [16] S. Korganbayev *et al.*, "PID controlling approach based on FBG array measurements for laser ablation of pancreatic tissues," *IEEE Trans. Instrum. Meas.*, pp. 1–1, 2021.
- [17] A. Mohammadi, L. Bianchi, S. Korganbayev, M. De Landro, and P. Saccomandi, "Thermomechanical Modeling of Laser Ablation Therapy of Tumors: Sensitivity Analysis and Optimization of Influential Variables," *IEEE Trans. Biomed. Eng.*, vol. 69, no. 1, pp. 302–313, Jan. 2022.
- [18] A. LeBrun, R. Ma, and L. Zhu, "MicroCT image based simulation to design heating protocols in magnetic nanoparticle hyperthermia for cancer treatment," *J. Therm. Biol.*, vol. 62, pp. 129–137, 2016.
- [19] N. Manuchehrabadi and L. Zhu, "Development of a computational simulation tool to design a protocol for treating prostate tumours using transurethral laser photothermal therapy," *Int. J. Hyperth.*, vol. 30, no. 6, pp. 349–361, 2014.
- [20] P. Saccomandi *et al.*, "Theoretical Analysis and Experimental Evaluation of Laser-Induced Interstitial Thermotherapy in Ex Vivo Porcine Pancreas," *IEEE Trans. Biomed. Eng.*, vol. 59, no. 10, pp. 2958–2964, Oct. 2012.
- [21] H. H. Pennes, "Analysis of tissue and arterial blood temperatures in the resting human forearm," *J. Appl. Physiol.*, 1998.
- [22] M. J. Borrelli, L. L. Thompson, C. A. Cain, and W. C. Dewey, "Time-temperature analysis of cell killing of BHK cells heated at temperatures in the range of 43.5°C to 57.0°C," *Int. J. Radiat. Oncol.*, vol. 19, no. 2, pp. 389–399, 1990.
- [23] C. T. Germer *et al.*, "Optical properties of native and coagulated human liver tissue and liver metastases in the near infrared range," *Lasers Surg. Med.*, 1998.